Bioactive Materials 3 (2018) 385–388

Contents lists available at ScienceDirect

Bioactive Materials

journal homepage: http://www.keaipublishing.com/en/journals/bioactive-materials/

Thin films of binary amorphous Zn-Zr alloys developed by magnetron co-sputtering for the production of degradable coronary stents: A preliminary study

Nathalie Annonay [a], Fatiha Challali [a], Marie-Noëlle Labour [b], Valérie Bockelée [a], A. Garcia-Sanchez [a], Florent Tetard [a], Marie-Paule Besland [c], Philippe Djemia [a], Frédéric Chaubet [b, *]

[a] Laboratoire de Science des Matériaux et des Procédés, UPR CNRS 3407, Université Paris 13, Sorbonne-Paris-Cité, Institut Galilée, 99 av J.B. Clément, 93430, Villetaneuse, France
[b] Laboratory for Vascular Translational Science, Inserm U1148, Université Paris 13, Université Paris-Diderot, Sorbonne-Paris-Cité, Institut Galilée, 99 av J.B. Clément, 93430, Villetaneuse, France
[c] Institut des Matériaux Jean Rouxel (IMN) UMR CNRS 6502, Université de Nantes, 2, rue de la Houssinière, B.P. 32229, 44322, Nantes Cedex 3, France

ARTICLE INFO

Article history:
Received 26 December 2017
Received in revised form
21 April 2018
Accepted 8 May 2018
Available online 26 May 2018

1. Introduction

Vascular stents are endo-prostheses that allow the restoration of blood flow in case of obstruction of a vessel. A stent usually consists of a corrosion-resistant metal such as Nitinol, 316L steel or a CoCr alloy [1]. Many studies have been undertaken for the production of polymer degradable stents [2,3] or metallic stents [4,5] and, among these, devices made of pure zinc or crystallized alloy based on zinc obtained by molding and extrusion are promising in terms of biodegradability, biocompatibility and mechanical properties [6], but also concerning the degradation rate of the stent which should to be effective until arterial remodeling and tissue healing are complete [5]. The objective of this preliminary study is the comparison of the degradation in simulated biological medium and the endothelial cytotoxicity of amorphous and crystallized thin ZnZr films according to their composition and structure. In this work, the thin layers were deposited on silicon substrates by magnetron co-sputtering. This technology is already used to make metal stents [7,8].

2. Materials and methods

The thin layers are made in the 4-source magnetron sputtering frame on silicon substrates. Two pure metal targets (Zinc and Zirconium) with a diameter of 2 inches and a thickness of 6 mm were used. A Schematic of the magnetron RF co-sputtering system and ZnZr plasma deposition are presented in Fig. 1.

2.1. Preparation of thin layers

ZnZr binary thin film metallic glasses with different compositions were prepared on silicon substrate by RF magnetron co-sputtering technique using Zn and Zr pure metal targets. The operating conditions were set at a base pressure lower than 10^{-5} Pa, a working pressure of 0.5 Pa and an Ar flow rate of 40 sccm. The sputtering time was varied with a sputtering power in 25–100 W and 25–200 W range for Zn and Zr targets respectively. The atomic content of Zn in the films increases with increasing the power ratio (P_{Zn}/P_{Zr}) applied to the two targets Zn and Zr. Deposition conditions and chemical composition are presented in Table 1.

2.2. Characterization of thin layers

The chemical composition of the thin layers after deposition was determined by energy dispersive X-ray spectroscopy (EDX) using a SEM-EDX LEICA S440. The acquisition was performed for a voltage of 15 kV and a probe current of 1000 pA. The thickness of the thin layers after deposition as well as their morphology after deposition and after degradation were obtained following the respective observation of their cross section and their surface under a scanning electron microscope with a field emission gun (SEM-FEG) ZEISS Supra 40VP. A voltage of 5 kV is used. The crystalline structure

* Corresponding author.
E-mail address: frederic.chaubet@univ-paris13.fr (F. Chaubet).
Peer review under responsibility of KeAi Communications Co., Ltd.

https://doi.org/10.1016/j.bioactmat.2018.05.004

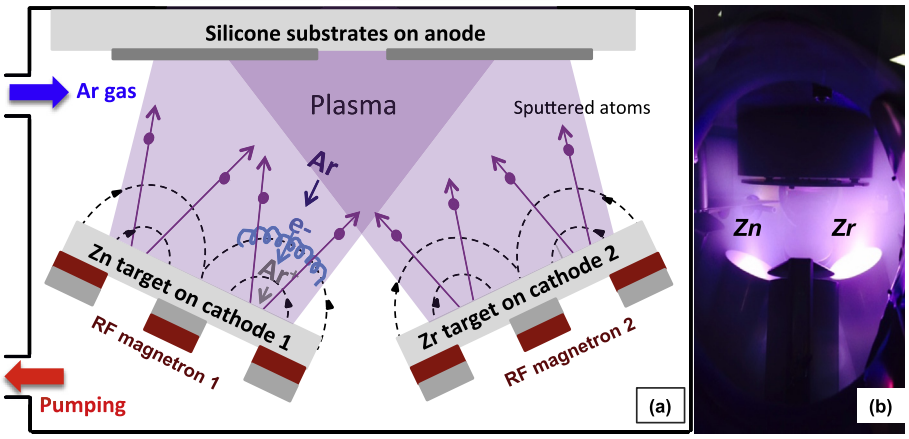

Fig. 1. (a) Schematic of the magnetron RF co-sputtering system and (b) image of ZnZr plasma deposition.

Table 1
Deposition parameters, film thickness, and chemical composition of the ZnZr thin films deposited by RF magnetron co-sputtering.

	Zn power (W)	Zr power (W)	P_{Zn}/P_{Zr} Power ratio	Deposition temp. (°C)	Annealing temp. (°C)	Film thickness (nm)[a]	Chemical Composition (EDX)[b]	
							Zn (% at.)	Zr (% at.)
ZnZr1	25	200	0.125	RT	–	330	16.1	83.9
ZnZr2	50	200	0.25	RT	–	334	29.8	70.2
ZnZr3	100	200	0.5	RT	–	291	37.3	62.7
ZnZr4	100	100	1	RT	–	275	55.8	44.2
ZnZr4-200	100	100	1	200	–	nd	53.1	46.9
ZnZr4-A300	100	100	1	–	300	275	55.3	44.7
ZnZr5	100	25	4	RT	–	276	91.7	8.3
ZnZr5-200	100	25	4	200	–	209	80.5	19.5
ZnZr5-A300	100	25	4	–	300	276	89.0	11.0

[a] ±10 nm.
[b] ±SD = 3–5%.

of the films was determined by the analysis of X-ray diffraction (XRD) spectra obtained using an Inel EQUINOX 1000 diffractometer in the Ω-2θ configuration equipped with a curved detector and an anticathode of Cobalt. The measurements were made for an angle of incidence of 2° and the line Kα1 of Cobalt (λ = 1.789010 Å). JCPDS data sets have been used for Zr hexagonal phases (JCPDS: 04-004-5064 and 04-006-2822) and Zn hexagonal phase (JCPDS: 04-008-6027). ZnZr thin layers were ex-situ investigated by X-Ray Photoelectrons Spectroscopy (XPS) performed with a Kratos Ultra Axis spectrometer using Al Kα radiation (photon energy 1486.6 eV) and 20 eV analyzer pass energy. The chemical composition of ZnZr films could be determined by the integration of Zr3d and Zn3p core level peaks, for Zr and Zn respectively.

2.3. Degradability of thin layers and corrosion test

The samples (0.7 cm 2) are each placed in 5 ml of simulated body fluid (SBF) [9] at 37 °C under gentle shaking. After 1 week or 2 weeks the samples are rinsed with distilled water and dried in an oven at 40 °C and their surface is observed under a scanning electron microscope. For corrosion study, electrochemical experiments were conducted in a standard three electrodes cell with 0.8 cm^2 of exposed area in the working electrode, having a platinum mesh as counter electrode and Ag/AgCl electrode as reference. The working electrolyte of simulated body fluid (SBF) was introduced in Teflon® cell at 20 °C. The corrosion test was evaluated by DC polarization curves. The immersion time of each sample was 1 h to investigate the corrosion current density (I_{corr}) and corrosion potential (E_{corr}). The voltage was scanned between −1 V and 0 V with a scan rate of 0.05 V/s. The corrosion current density (I_{corr}) was obtained using Tafel extrapolation technique at ± 50 mv around open circuit potential. DC test was carried by Autolab PGSTAT. For each sample, two replications were performed. An anodization of the two samples ZnZr4 and ZnZr5 made at RT were conducted at 1 V during 1 h in SBF.

2.4. Cytotoxicity test

Human umbilical cord vein endothelial cells (HUVEC-Cs, ATCC) were seeded on the samples at a density of 2×10^4 cells/cm^2 in DMEM containing 10% FBS and 1% Antibiotic-Antimycotic. Cell viability was analyzed after 72 h using a resazurin based metabolic activity assay (In vitro Toxicology Assay Kit, Sigma Aldrich®) following the manufacturer's instructions. Experiments were carried out according to the ISO 10993-5: 2009 standard applicable to the MTT and resazurin tests. The fluorescence intensity, proportional to the cell number, was normalized to control cells seeded in multi-well plate. Experiments were performed in triplicate with n = 8. Statistics were performed using One-way Anova and a Tukey post test.

3. Results and discussion

According to the model of Egami and Waseda [10] and the work of Braic and co-workers [11] we have established that amorphous ZnZr alloys could be synthesized for zirconium concentrations between 23% at. and 70% at. Table 1 gathers the experimental conditions, composition and thickness of ZnZr films for zinc

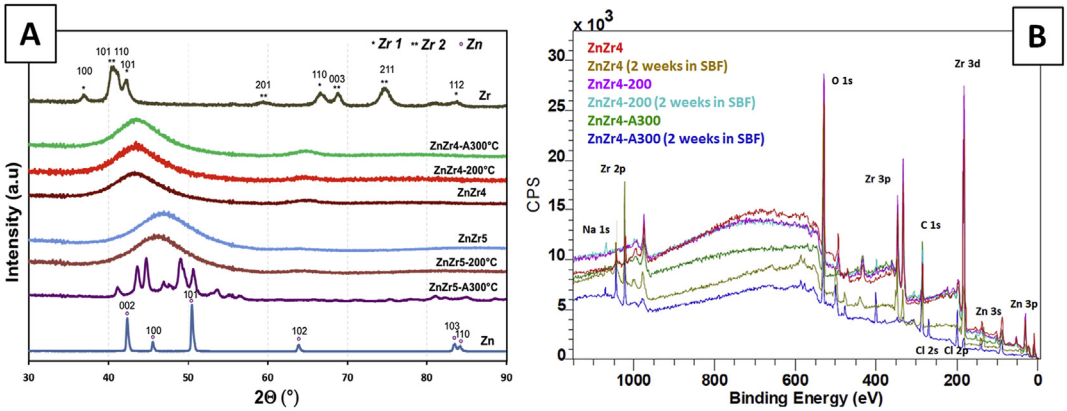

Fig. 2. (A) XRD patterns of thin films of Zn, Zr and ZnZr4 and ZnZr5 samples as well as deposited by RF magnetron co-sputtering at room temperature (RT). (*) and (**) depict Zr hexagonal phases (JCPDS: 04-004-5064 and 04-006-2822 respectively) and (o) Zn hexagonal phase (JCPDS: 04-008-6027). Only films with Zn content from 29.8% at. were obtained in the amorphous state. (B) XPS profiles of ZnZr4 samples before and after 2 weeks in SBF.

concentrations above 30% at. obtained from EDX measurements and SEM images respectively. All films were obtained in the amorphous state at room temperature and at 200 °C for ZnZr4 and ZnZr5 samples. After annealing at 300 °C, only ZnZr5 was recristallized. XRD analyses of the ZnZr4 and ZnZr5 samples are presented on Fig. 2A (see Electronic Supplementary Information for XRD of the other samples). The degradation behavior of the samples immersed in SBF [9] for 1 week and 2 weeks was studied. XPS analysis have been performed and XPS profiles of the ZnZr4 samples are presented on Fig. 2B as an example. Zinc and zirconium were evidenced at the surface (5–10 nm depth) as well as contaminants such as oxygen and carbon. In agreement with the EDX analysis, the Zn/Zr atomic ratio was higher for the ZnZr5 samples than for the ZnZr4 samples. Likewise, the zinc content at the surface was confirmed as lower after a deposit at 200 °C than after a deposition at ambient temperature. However, surfaces must be carefully eroded to remove contaminants in order to get a relevant quantitative analysis, what is a long and tricky process with thin layers and almost impossible to apply to the degraded samples (see Fig. 3). Anyway, in a first rough approximation, a trend towards a lower zirconium content of the degraded samples was estimated by XPS indicating a preferential solubilization of this element in the SBF. The examination of the surface morphology by SEM revealed that only ZnZr4 and ZnZr5 alloys (zinc concentration from 55.8% at.) were deteriorated over two weeks (Fig. 3B and D). Corrosion tests performed in SBF by potentiometry at room temperature on ZnZr4 and ZnZr5 samples evidenced a high sensitivity to corrosion. Due to the surface condition after degradation, it was not possible to establish the corrosion rates (CR) but the CR(ZnZr5)/CR (ZnZr4) ratio was estimated to about 10 (see ESI). The cytotoxicity of thin films to endothelial cells of the Human umbilical cord vein (HUVECs) was evaluated on both samples. The amorphous and crystallized ZnZr5 samples were found to be non-cytotoxic as well as the pure Zn sample, and the cells appeared to prolifer more on the surface of the crystallized samples (Fig. 4). On the contrary pure Zr sample and ZnZr4 samples were found cytotoxic. Since the chemical composition did not change significantly after annealing, the behavior of the HUVECs could be influenced by the crystalline

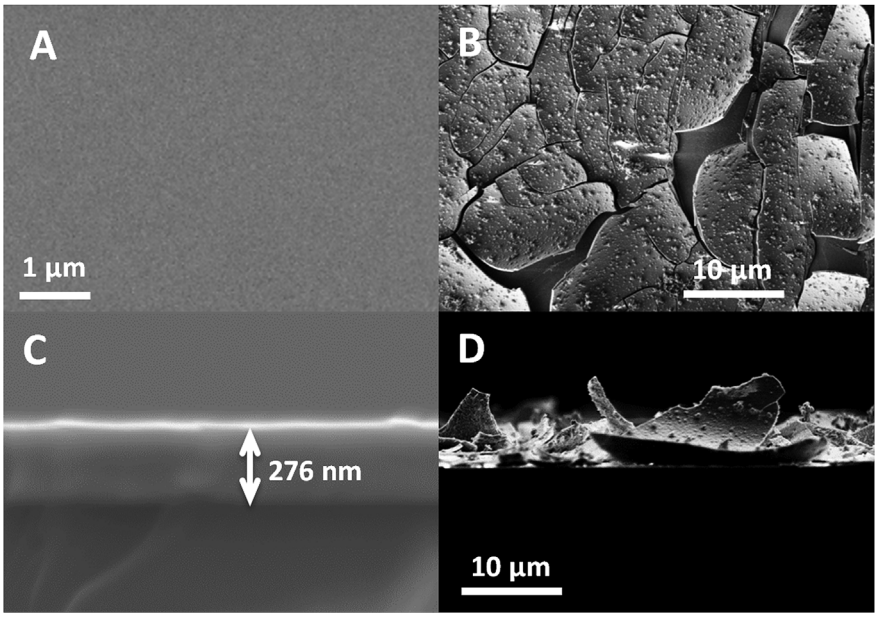

Fig. 3. SEM imaged of ZnZr5 thin layer. Top plan view of the film as deposited (A) and after 2 weeks in SBF (B). Cross-section views of the same sample film as deposited (C) and after 2 weeks in SBF. ZnZr4 samples presented a similar aspect (data not shown).

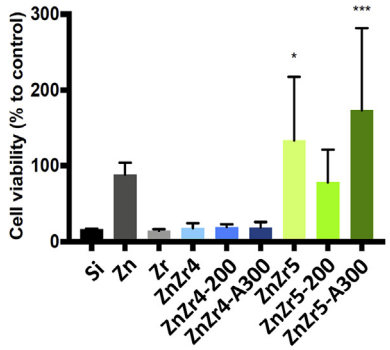

Fig. 4. Resazurin in vitro HUVECs viability assay with ZnZr4 and ZnZr5 samples (see Table 1). A comparison is made with the deposition substrate (silicon) and pure zinc and zirconium films. Experiments were performed in triplicate with n = 8. Statistics were performed using One-way Anova and a Tukey post test. Results with ZnZr5 RT and ZnZr5 A300 are significantly different from all except Zn and ZnZr5 200 (*$p < 0.01$ and ***$p < 0.0001$).

nature of the material. Eventually, the highest proportion of Zr in ZnZr4 would explain its cytotoxicity compared with ZnZr5.

4. Conclusion

Thin amorphous and crystallized films of ZnZr alloy were obtained by magnetron co-sputtering with zinc compositions varying from 16 to 92% at. Electronic microscopy and corrosion studies have evidenced a rapid degradation by corrosion of the samples richest in zinc (from 56% at.) in simulated body fluid over two weeks. A first examination of cytotoxicity to human endothelial cells indicates good cytocompatibility of both amorphous and crystalline films with zinc content above 80% at. Such thin metallic glass layers obtained by magnetron co-sputtering of zinc and zirconium on a sacrificial substrate could be considered for the development of novel Zn-based vascular degradable stent as in the case of tubular vascular implants in titanium-nickel alloy developed by Habijan et al. [8].

Appendix A. Supplementary data

Supplementary data related to this article can be found at https://doi.org/10.1016/j.bioactmat.2018.05.004.

References

[1] G.G. Stefanini, R.A. Byrne, S. Windecker, A. Kastrati, State of the art: coronary artery stents - past, present and future, Eurointervention 13 (6) (2017) 706–716.
[2] S.H. Im, Y. Jung, S.H. Kim, Current status and future direction of biodegradable metallic and polymeric vascular scaffolds for next-generation stents, Acta Biomater. 60 (2017) 3–22.
[3] H.Y. Ang, H. Bulluck, P. Wong, S.S. Venkatraman, Y. Huang, N. Foin, Bioresorbable stents: current and upcoming bioresorbable technologies, Int. J. Cardiol. 228 (2017) 931–939.
[4] K. Yang, C.C. Zhou, H.S. Fan, Y.J. Fan, Jiang Q. Song, P. Fan HY, Y. Chen, X.D. Zhang, Bio-functional design, application and trends in metallic biomaterials, Int. J. Mol. Sci. 19 (1) (2018) 4561–4573.
[5] E. Mostaed, M. Sikora-Jasinska, A. Mostaed, S. Loffredo, A.G. Demir, B. Previtali, D. Mantovani, R. Beanland, M. Vedani, Novel Zn-based alloys for biodegradable stent applications: design, development and in vitro degradation, Journal of the Mechanical Behavior of Biomedical Materials 60 (2016) 581–602.
[6] P.K. Bowen, E.R. Shearier, S. Zhao, R.J. Guillory II, F. Zhao, J. Goldman, J.W. Drelich, Biodegradable metals for cardiovascular stents: from clinical concerns to recent Zn-alloys, Advanced Healthcare Materials 5 (2016) 1121–1140.
[7] N.M. Roth, A Method for Fabricating a Stent or Other Medical Device by Creating a Free Standing Thin Film of Metal, 2003. United States Patent, 6,527,919.
[8] T. Habijan, R.L. De Miranda, C. Zamponi, E. Quandt, C. Greulich, T.A. Schildhauer, M. Koller, The biocompatibility and mechanical properties of cylindrical NiTi thin films produced by magnetron sputtering, Mater. Sci. Eng. C 32 (8) (2012) 2523–2528.
[9] T. Kokubo, H. Takadama, How useful is SBF in predicting in vivo bone bioactivity? Biomaterials 27 (15) (2006) 2907–2915.
[10] T. Egami, Y. Waseda, Atomic size effect on the formability of metallic glasses, J. Non-Cryst. Solids 64 (1–2) (1984) 113–134.
[11] M. Braic, V. Braic, A.N. Vladescu, C. Zoita, M. Balaceanu, Solid solution or amorphous phase formation in TiZr-based ternary to quinternary multi-principal-element films, Prog. Nat. Sci.: Mater. Int. 24 (4) (2014) 305–312.